International Journal of Astrobiology 9 (3): 137–146 (2010)
doi:10.1017/S147355041000011X © Cambridge University Press 2010

Putative fossil life in a hydrothermal system of the Dellen impact structure, Sweden

Paula Lindgren[1], Magnus Ivarsson[1], Anna Neubeck[1], Curt Broman[1], Herbert Henkel[2] and Nils G. Holm[1]

[1]*Department of Geological Sciences, Stockholm University, Stockholm S-106 91, Sweden*
e-mail: paula.lindgren@geo.su.se
[2]*Kungliga Tekniska Högskolan, Stockholm S-100 44, Sweden*

Abstract: Impact-generated hydrothermal systems are commonly proposed as good candidates for hosting primitive life on early Earth and Mars. However, evidence of fossil microbial colonization in impact-generated hydrothermal systems is rarely reported in the literature. Here we present the occurrence of putative fossil microorganisms in a hydrothermal system of the 89 Ma Dellen impact structure, Sweden. We found the putative fossilized microorganisms hosted in a fine-grained matrix of hydrothermal alteration minerals set in interlinked fractures of an impact breccia. The putative fossils appear as semi-straight to twirled filaments, with a thickness of 1–2 μm, and a length between 10 and 100 μm. They have an internal structure with segmentation, and branching of filaments occurs frequently. Their composition varies between an outer and an inner layer of a filament, where the inner layer is more iron rich. Our results indicate that hydrothermal systems in impact craters could potentially be capable of supporting microbial life. This could have played an important role for the evolution of life on early Earth and Mars.

Received 21 October 2009, accepted 14 March 2010, first published online 23 April 2010

Key words: early Earth, early Mars, hydrothermal system, impact structure, microfossils.

Introduction

Impact-generated hydrothermal systems

Impacts in water-bearing targets can generate hydrothermal systems. A large impact produces a central uplift and impact melts, which are sources of heat. The impact also creates deep fractures in the target, which provide pathways for water to flow through the rock (Newsom 1980; Naumov 2002). Evidence of impact-generated hydrothermal activity has been identified in over a third of the ca 170 impact craters here on Earth (Naumov 2002). Impact-generated hydrothermal systems are also likely to have occurred on Mars (Newsom 1980). Hydrothermal systems can prevail in impact craters for thousands of years, such as in the ca 455 Ma Kärdla impact structure, Estonia (Jõeleht *et al*. 2005) and in the ca 39 Ma Haughton impact structure, Canada (Parnell *et al*. 2007), and for substantially longer periods (up to a million years) in very large craters, such as in the ca 1850 Ma Sudbury impact structure, Canada (Ames *et al*. 1998). Impact-generated hydrothermal systems are often suggested as suitable habitats for primitive life (Rathbun & Squyres 2002; Versh *et al*. 2006). There are no active impact-generated hydrothermal systems on Earth today, but microorganisms thrive in hydrothermal settings of volcanic regions, for instance in hot springs onshore and around marine hydrothermal vents (Brock 1978; Corliss *et al*. 1979; Corliss *et al*. 1981). In addition, a fossil biota in volcanic-induced hydrothermal settings is preserved in the geological record (Little *et al*. 1998; Geptner *et al*. 2005). However, fossil evidences of biological colonization in impact-generated hydrothermal systems are seldom described in the literature. To our knowledge, there are so far only two reported occurrences of this, namely possible microbial forms on hydrothermal alteration minerals from the ca 15 Ma Ries impact crater, Germany (Glamoclija *et al*. 2007), and fossilized extracellular polymeric substances (EPSs) of microorganisms that could have lived in a hydrothermal system of the ca 377 Ma Siljan impact structure, Sweden (Hode *et al*. 2008). Further, recent chemical data from sulphur isotopes in the Haughton impact crater, Canada, indicate rapid colonization of the impact crater by thermophilic microorganisms (Parnell *et al*. 2010). We analysed impact breccia from the Dellen impact structure in Sweden, and in the samples we detected the putative microfossils that are described in this paper.

The Dellen impact structure

The Dellen impact structure is located in east-central Sweden (Fig. 1), and was formed about 89 million years ago (Deutsch *et al*. 1992). An impact origin for Dellen was confirmed by Svensson (1968) through the identification of shocked quartz.

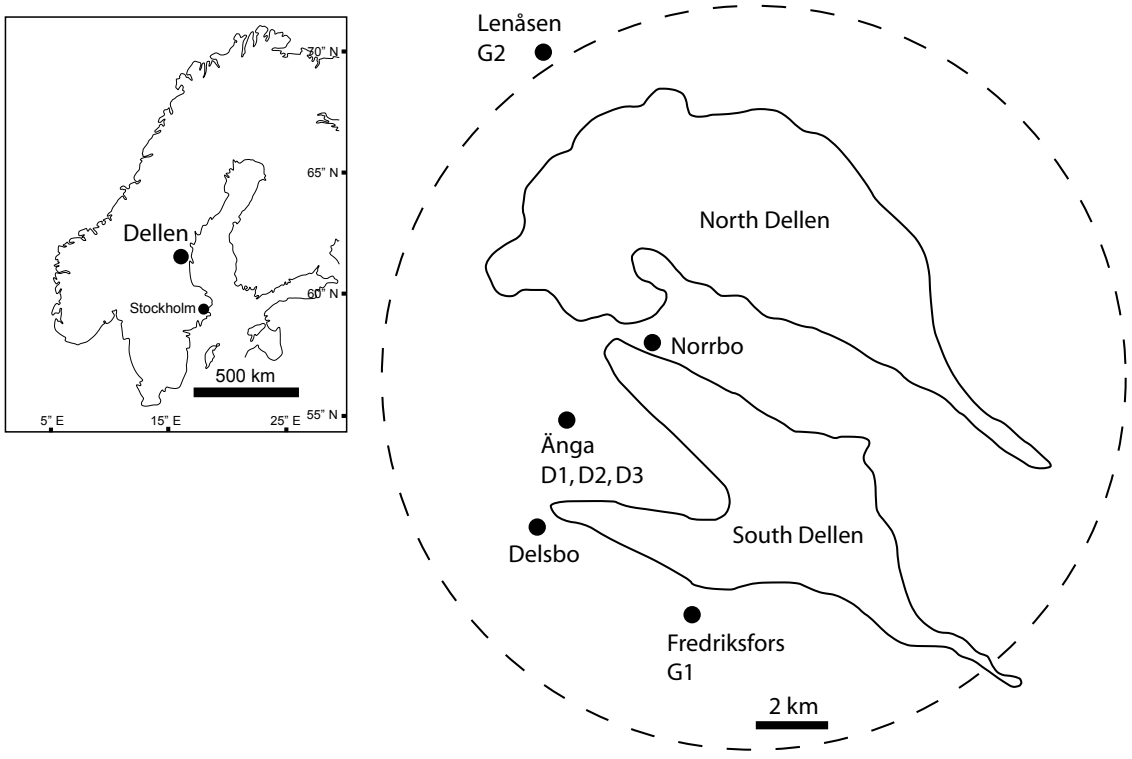

Fig. 1. A map of Scandinavia showing the location of the Dellen impact structure, and a map of the Dellen lakes with a dashed circle showing the outline of the impact structure. The sample localities are marked on the map.

Dellen is a complex impact structure, i.e., it has a central uplift. The present diameter of the structure is ca 20 km. A large part of the structure is buried under a thick moraine cover, and most impactite material is only available as loose blocks and boulders in the moraine. Dellen contains a large volume of both coherent melt (vernacular name: Dellenite) and melt-rich breccia (suevite). Aeromagnetic measurements show the present extent of melt-bearing impactites in Dellen to be ca 9 km in diameter and 200–500 m thick (Henkel 1992). The melt-bearing impactites and the central uplift were sources of heat driving the hydrothermal system. The melt-bearing impactites overlie lithic impact breccia and fractured basement rocks. The target bedrock of Dellen is largely composed of granitoids (Ljusdal granite) of variable metamorphic grade, and the target is intensively fractured due to the impact (Henkel 1992). Fractured basement rocks surrounding impact craters can extend to great depths below impact melt sheets. For instance, in the ca 24 km diameter Ries impact crater in Germany, the bedrock may be fractured to at least 3 km below the crater (Dence *et al*. 1977). The ca 15 Ma Ries impact crater is a relatively young and well-preserved structure, and with a similar diameter to Dellen. Fractured basement rocks below craters allow groundwater to travel from a large area surrounding the crater to the hot hydrothermal circulation system. The duration of the hydrothermal system in the Dellen crater is not established yet, but it can be estimated to about 5000 years, based on previous models of the duration of a hydrothermal system in the similar-sized Haughton crater in Canada (Parnell *et al*. 2007). Haughton has a diameter of about 23 km and Dellen has a present diameter of about 20 km. Further similarities between the two craters that would allow such a comparison are that both Haughton and Dellen contain large volumes of melt-bearing impactites and central uplifts. These are the heat sources necessary to drive the hydrothermal system in impact craters. A hydrothermal system of 5000 years would be enough time for colonization. However, colonization can of course not take place until the system has cooled to favourable temperatures (Versh *et al*. 2006). Recent data of sulphur-isotope signatures from the Haughton crater, which is similar in size to Dellen, indicate that colonization can occur within the lifetime of such a moderately-sized, impact-generated hydrothermal system (Parnell *et al*. 2010).

Samples and methods

Since most of the Dellen structure is currently buried under a thick soil cover, the samples in this study were largely collected at a locality with abundant large blocks and boulders of impactites (Lindström & von Dalwigk 2002) (Fig. 1, Ånga). The Dellen impactites include both melt-bearing impactites (Dellenite and suevite) and non-melt-bearing (lithic) impact breccia. We focused our analyses on lithic impact breccia and, as a comparison, the crystalline target granite. The target granite was collected at localities that are affected by a large-scale impact fracturing (Henkel 2009 personal communication), but our samples of the target granite do not show any obvious impact effects on a smaller hand specimen scale. We examined three different samples of lithic impact breccia from one locality (Ånga), and two different samples

https://doi.org/10.1017/S147355041000011X Published online by Cambridge University Press

Table 1. *Description, locality, number of thin sections and occurrence of filaments in samples from Dellen*

Sample	Description	Locality	Thin sections*	Occurrence of filaments
DL1	Lithic impact breccia: monomictic, clast-supported, granitic composition.	Änga	2**	Yes
DL2	Lithic impact breccia: monomictic, clast-supported, granitic composition.	Änga	1	No
DL3	Lithic impact breccia: monomictic, clast-supported, granitic composition.	Änga	1	No
DG1	Ljusdal granite: crystalline target rock without any small-scale obvious impact effects. Medium grained, massive, granitic composition.	Fredriksfors	1	No
DG2	Ljusdal granite: crystalline target rock without any small-scale obvious impact effects. Medium grained, massive, granitic composition.	Lenåsen	1	No

* The thin sections are polished and have a thickness of 30 μm.
**One polished thin section and one 200 μm thick doubly polished wafer.

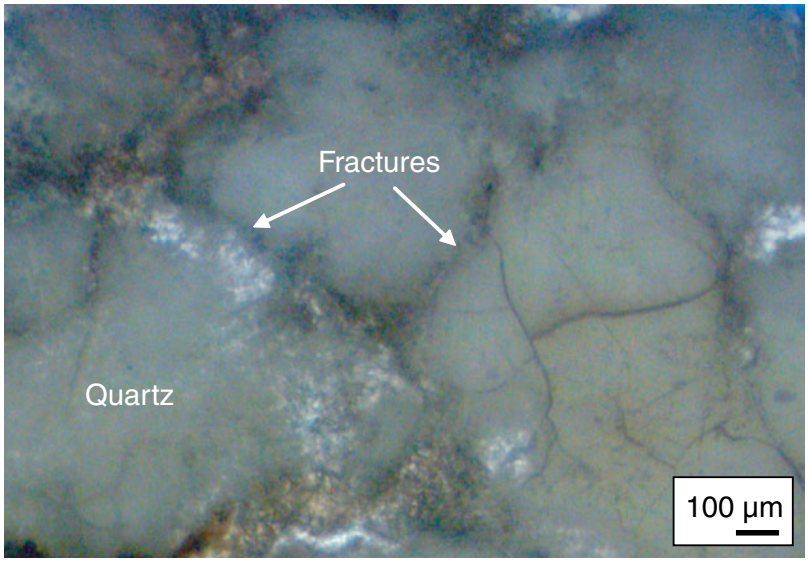

Fig. 2. A photomicrograph in plane-polarized light of interconnected fractures in lithic impact breccia from Dellen.

of the crystalline target rock, Ljusdal granite, from two different localities (Table 1). The samples were prepared as polished thin sections with a thickness of 30 μm and as a 200 μm thick doubly polished wafer (Ivarsson 2006). The samples were analysed with a standard petrographic microscope and with an XL30 environmental scanning electron microscope (ESEM) with a field emission gun (XL30 ESEM-FEG) at Stockholm University, Sweden. The ESEM was equipped with an Oxford x-act energy dispersive spectrometer (EDS), a back-scatter electron detector (BSE) and a secondary electron detector (SE). The samples were not carbon coated prior to analyses in a low vacuum. The acceleration voltage was 20 kV and the instrument was calibrated with a cobalt standard.

Results

Setting of filamentous structures

The filamentous structures occur in one out of three different samples of impact breccia (Table 1). Within this sample they are widespread and abundant. The filaments do not occur in the samples of crystalline target granite. The filaments occur in assemblages throughout interlinked and sealed fractures of the severely fractured impact breccia (Fig. 2). The thicknesses of the fractures vary from 10 to 700 μm (Fig. 3(a)). The fractures are filled with a fine-grained mixture of hydrothermal alteration minerals. The alteration minerals are too small and fragile to analyse individually in the ESEM. Therefore, the bulk composition of the fracture fill in 15 different areas of about 2 μm × 2 μm each were analysed qualitatively in the ESEM (Table 2). The chemical composition of the fracture fill and the fine-grained texture of these alteration minerals indicate that the fractures are mostly filled with clay minerals and zeolites. Clay minerals and zeolites are indicative of a low-temperature hydrothermal alteration (e.g. Schiffman & Southard 1996; Utada 2001). The impact breccia has a granitic composition, i.e., mainly quartz and feldspars, and is most likely former Ljusdal granite, which is the crystalline target of Dellen. The impact breccia is composed of angular granitic fragments ranging in size from a few millimetres to a few centimetres, most of them with a size of less than 5 mm.

Morphology of filamentous structures

The filaments appear as semi-straight to twirled structures (Fig. 3(b)). In many cases they display a segmented,

https://doi.org/10.1017/S147355041000011X Published online by Cambridge University Press

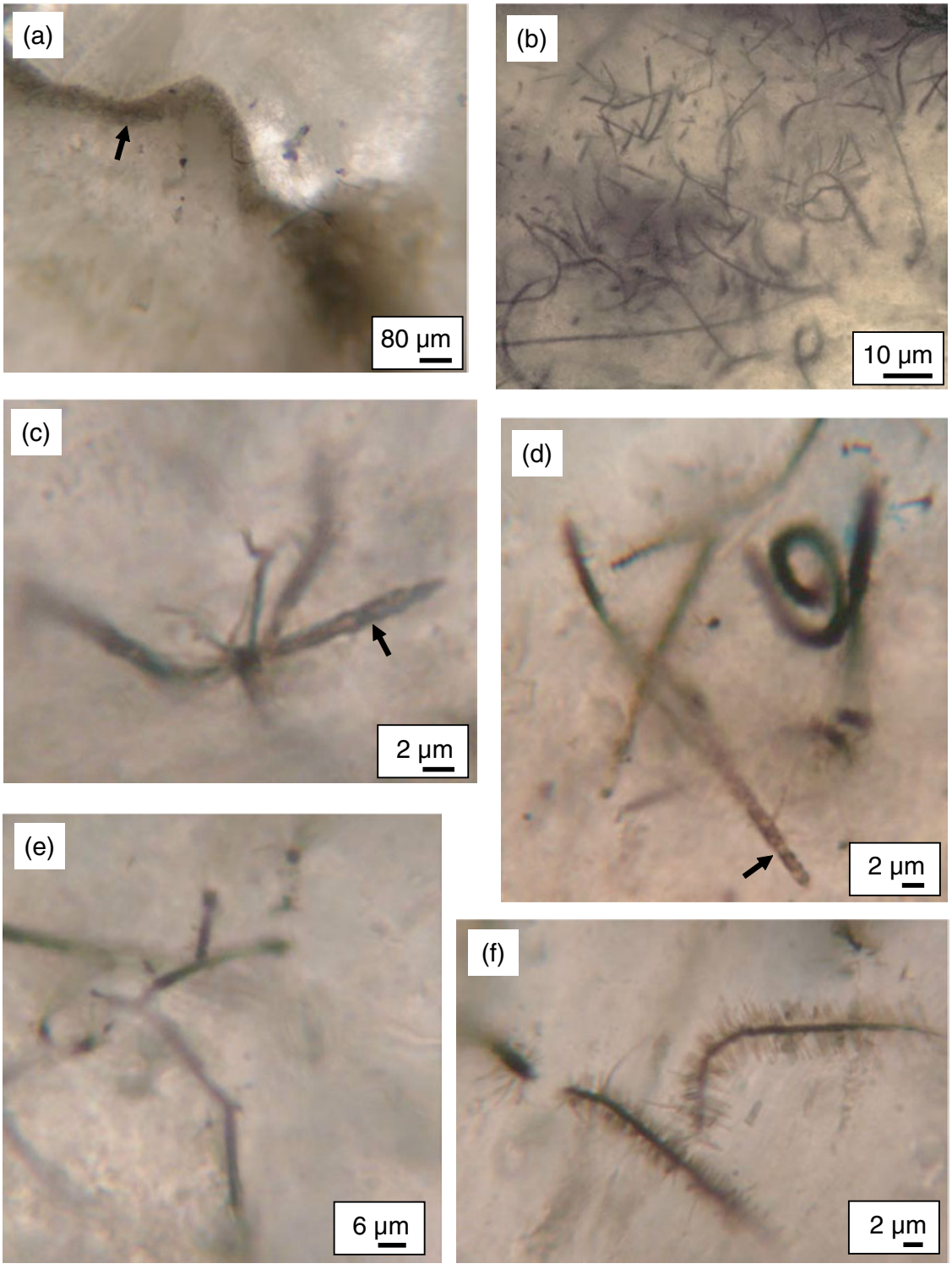

Fig. 3. (a) An overview photomicrograph in plane-polarized light of a fracture in lithic impact breccia filled with hydrothermal alteration minerals and filamentous structures (arrow). (b) A closer photomicrograph in plane-polarized light of an assemblage of filamentous structures located in fractures of the impact breccia. The filaments appear as semi-straight to twirled structures. (c) A photomicrograph in plane-polarized light of a star-shaped filamentous structure. Note segmentation (arrow). (d) A photomicrograph in plane-polarized light of a coiled filament (dark). Note also segmentation (arrow). (e) A photomicrograph in plane-polarized light of branching filaments. (f) A photomicrograph in plane-polarized light of filaments enclosed by fibrous structures.

star-shaped and branched morphology. They are sheeted, which means that they are composed of an inner and an outer part, where the inner part is more iron rich (see below). The thicknesses of the filaments are consistently 1–2 µm, and their lengths vary from about 10 to 100 µm. The segmented morphology (Figs 3(c) and (d)) is visible as a colour variation

https://doi.org/10.1017/S147355041000011X Published online by Cambridge University Press

Table 2. *The elemental composition of the fracture fill surrounding the filaments* (*Fig. 5*). *The composition is obtained by EDS analyses in the ESEM of 15 different areas of about 2 μm × 2 μm each, in the fracture fill. The values are normalized and given in weight%*

Normalized fracture fill	wt% C	Na	Al	Si	K	Fe	O	Total
	1.8	1.27	8.47	29.84	9.52	0.28	48.83	100
		1.36	8.81	32.17	9.87	0.57	47.22	100
	2.56	1.31	8.34	28.92	9.01	0.25	49.6	100
	2.93	1.15	8.21	28.47	9.08	0.25	49.91	100
		1.08	9.22	31.87	10.75		47.08	100
	1.42	1.27	8.49	30.41	9.66	0.24	48.51	100
	2.39	1.24	8.45	29.12	9.09	0.25	49.46	100
		1.35	9.11	31.82	10.29	0.35	47.08	100
	1.68	1.27	8.66	29.9	9.46	0.28	48.74	100
	1.68	1.27	8.66	29.9	9.46	0.28	48.74	100
		1.38	9.32	31.81	10.01	0.29	47.18	100
		1.33	9.38	31.58	10.29	0.37	47.05	100
		1.74	9.24	31.43	9.84	0.77	46.98	100
	3.55	1.44	8.18	27.43	8.69	0.3	50.4	100
	1.75	1.42	8.8	29.64	9.22	0.36	48.8	100

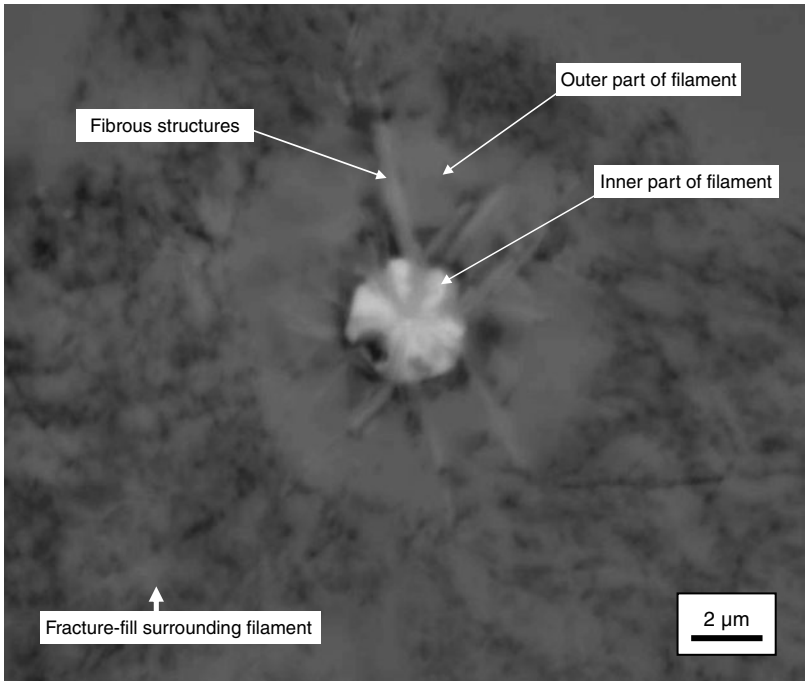

Fig. 4. A close-up ESEM micrograph showing a transversal cross-section of a filament, with an inner and outer layer. Fibrous structures are radiating out from the centre of the filament. The filament is enclosed in fracture-filling hydrothermal alteration minerals (clay minerals and zeolites).

(in optical microscopy, plane-polarized light) from brown-red to black within a single filament. The star-shaped filaments are divided into six or seven filaments that all originate from the same centre. Here, the individual filaments are all of similar length and they display segmentation (Fig. 3(c)). Branching of the filaments occurs frequently and not only in single steps, but also in multiple, repeated steps, like the initiating steps of a dendritic pattern (Fig. 3(e)). Some of the filamentous structures are covered by a fibrous material that radiates perpendicular to the filamentous structures in a 360° fashion (Fig. 3(f)). These fibres are ca 5–10 μm in length and less than 1 μm in diameter. In cross-section it is possible to see that these fibres originate in the inner parts of the filaments and stretch through both the inner and outer parts of the filaments (Fig. 4). In the light microscopy image of Fig. 3(f), it can be seen that the fibres extend outside the filament. This is not visible in the BSE-ESEM micrograph of Fig. 4. This is because the BSE-ESEM micrograph in Fig. 4 records the difference in atomic mass of the various components at the surface of the specimen. It is possible that the fibrous

https://doi.org/10.1017/S147355041000011X Published online by Cambridge University Press

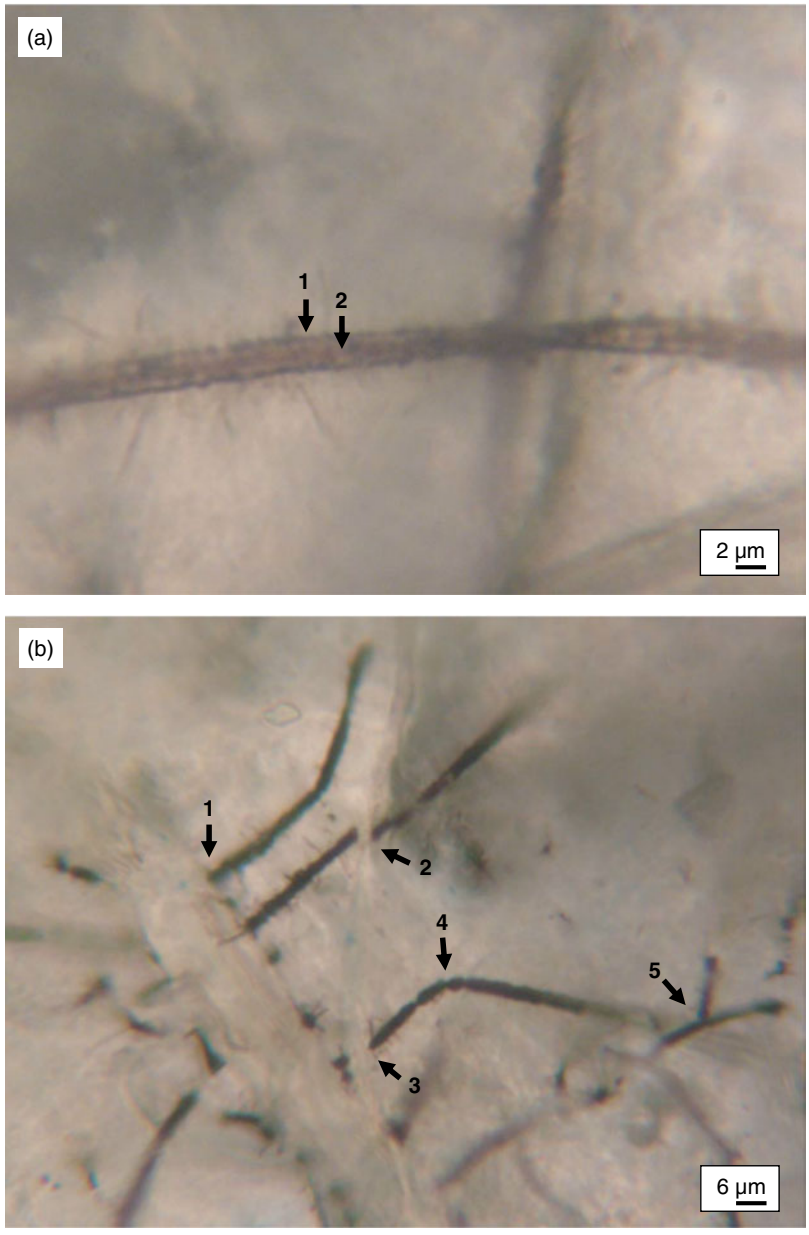

Fig. 5. (a) A photomicrograph in plane-polarized light of a sheeted filament. Two arrows pointing to (1) the outer layer and (2) the inner layer. (b) A photomicrograph in plane-polarized light of filaments that are cut off by the fracture-filling hydrothermal alteration minerals (arrows 1–3). Note also segmentation (arrow 4) and branching (arrow 5).

structures are also extending from the filament shown in Fig. 4, but they are not at the surface of the sample, and/or have a similar atomic mass as the surrounding fracture fill, and hence are not visible on the ESEM micrograph, as they are in the optical image in Fig. 3(f). The filaments are sheeted. This means that they have distinguished inner and outer filamentous walls (Fig. 5(a)). The inner part has a reddish appearance in light microscopy compared to the outer part, which is almost transparent. In the ESEM the inner part has a bright appearance compared to the outer part (Fig. 4). The filaments are sometimes cut off by the fracture-filling hydrothermal alteration minerals (Fig. 5(b)).

Composition of filamentous structures

The filamentous structures are largely composed of oxygen, silica and iron, with some aluminium and potassium, and minor amounts of sodium, magnesium and manganese (Tables 3 and 4). The filamentous structures are sheeted with very distinguished inner and outer filamentous walls (Fig. 5(a)). This visual difference between the inner and outer parts is due to the difference in Fe, Mg and Mn content. The inner part is much more enriched in Fe (Table 3) than the outer part (Table 4), and the outer part almost completely lacks Mg and Mn.

https://doi.org/10.1017/S147355041000011X Published online by Cambridge University Press

Table 3. *The elemental composition of the inner part of filaments* (*Fig. 5*). *The composition is obtained by EDS analyses in the ESEM with three different point analyses each, in 10 different filaments* (*1–10, same as in Table 4*). *The values are normalized and given in weight %*

Normalized Inner part of filaments	wt % C	Na	Mg	Al	Si	Cl	K	Mn	Fe	O	Total
1	1.6	0.45	0.46	5.71	17.28		4.87	0.33	27.08	42.21	100
1		0.54	0.87	6.27	18.54		5.03	0.39	27.79	40.55	100
1		0.64	0.65	6.68	21.18	0.18	6.14		22.77	41.76	100
2		0.81	0.59	5.91	18.37		5.25	0.26	28.55	40.27	100
2		0.68	0.78	6.25	19.25		5.17	0.37	26.64	40.86	100
2		0.73	1.01	6.82	21.8		6.13	0.29	21.02	42.19	100
3	1.96	0.63	0.85	6	17.74		4.95	0.21	24.53	43.14	100
3		0.75	0.68	6.51	20.65		6.14		23.78	41.49	100
3		0.73	0.83	6.92	21.59	0.17	6.31	0.23	21.2	42.02	100
4	2.4	0.7	0.5	6.45	19.13	0.16	5.35	0.21	20.6	44.5	100
4	1.61	0.59	0.56	5.98	16.98		4.42	0.28	27.33	42.25	100
4	1.89	0.67	0.53	5.98	17.16		4.64	0.31	26.08	42.73	100
5	0.67		0.8	6.87	20.76		6.67	0.28	22.36	41.58	100
5	2.61	0.5	0.74	5.77	16.74		4.97	0.34	24.73	43.58	100
5		0.61	0.85	6.59	19.42		5.83	0.27	25.46	40.97	100
6		0.67	1.1	6.96	19.81		5.59	0.31	24.22	41.35	100
6		0.64	0.83	6.75	20.19		6.03	0.34	23.85	41.36	100
6	1.44	0.62	0.64	6.68	20.28		6.21	0.26	20.27	43.59	100
7	1.73	0.52	1.09	5.56	16.19		4.32	0.26	28.31	42.02	100
7		0.64	1.05	5.85	16.55		4.41	0.41	31.54	39.55	100
7		0.82	0.8	6.4	18.5		4.91	0.25	27.75	40.58	100
8	2.28	0.53	0.82	6.47	19.55	0.19	5.94	0.23	19.53	44.48	100
8	1.77	0.47	0.92	6.15	17.82		5.18	0.38	24.4	42.91	100
8	1.99	0.58	0.9	5.46	15.8		4.39	0.37	28.37	42.14	100
9	2.23	0.67	0.83	6.37	18.59		5.05	0.23	21.94	44.09	100
9	1.55	0.73	0.9	6.95	20.66	0.18	5.92	0.2	18.83	44.07	100
9		0.73	0.85	6.81	20.19		5.65	0.23	24.11	41.45	100
10		0.64	1.26	6.97	20.88	0.19	6.45		21.87	41.75	100
10	1.88	0.56	1.01	6.5	19.55		6.03	0.19	20.33	43.94	100
10	1.52	0.6	1.05	6.44	19.71		5.96	0.22	21.04	43.46	100

In some instances, the filaments and the fracture fill, as well as other phases in the sample outside the fractures, contain up to about 3 wt % carbon and trace amounts of chlorine. The sample was not carbon coated prior to analyses in the ESEM. The carbon and chlorine are most likely contaminants, i.e., not indigenous to the sample, as the glue of the polished sections contains carbon and chlorine. To further test this, an un-coated polished block (i.e., a block that was not in contact with glue) of the same sample was tested for carbon in the ESEM. Carbon was also detected here, but only in trace amounts, i.e., less than 1 %. This further indicates that the higher concentrations of carbon that were detected in the thin sections reflect that the carbon is contamination from the glue. In addition to analysing for carbon in the ESEM, total organic carbon (TOC) analyses were performed on powdered lithic impact breccia containing filaments, and on the granitic target rock (Table 5). The material was analysed for TOC with a Carlo Erba NC2500 carbon analyser at Stockholm University. The analysis was conducted on powdered material that had not been in contact with glue, or carbon coated. All of the samples yielded low values of TOC; from 0.18 % in the target granitoid to 0.42 % in the lithic impact breccia (Table 5). The TOC analyses confirm that carbon is not present in substantial amounts in either the target or the breccia, so if the filaments have a biogenic origin, carbon was not preserved in significant amounts.

Discussion

Origin of the filamentous structures

The filamentous structures observed in Dellen could have a biogenic origin, but there is also a possibility that they formed abiogenically. Most of the criteria listed for establishing biogenicity of putative fossilized microorganisms involve microfossils in sedimentary rocks with organic remains preserved (Schopf & Walter 1983; Schopf 1999; Gibson *et al*. 2001). The putative Dellen microfossils are mineralized with no significant organic remains, and found in fractures sealed by hydrothermal precipitates. This means that only certain criteria previously used on organic microfossils, such as morphology and size distribution, apply to the filamentous structures in Dellen. Another feature that makes the filamentous structures in Dellen congruent with biogenicity is their occurrence and distribution in a hydrothermal system: a geologic environment compatible with life.

The filamentous structures from Dellen bear close resemblance to encrusted and fossilized microorganisms previously found in samples from volcanism-induced hydrothermal

https://doi.org/10.1017/S147355041000011X Published online by Cambridge University Press

Table 4. *The elemental composition of the outer part of filaments* (*Fig. 5*). *The composition is obtained by EDS analyses in the ESEM with three different point analyses each, in 10 different filaments* (*1–10, same as the filaments in Table 3*). *The values are normalized and given in weight %*

Normalized Outer part of filaments	wt % C	Na	Mg	Al	Si	Cl	K	Mn	Fe	O	Total
1	1.88	0.82		8.32	29.09		10		1.41	48.48	100
1	1.56	0.97		8.03	28.66		10.18		2.94	47.65	100
1		0.96	0.53	8.02	27.13	0.21	8.45		9.95	44.74	100
2	1.56	0.92		7.97	27.7		9.06		5.48	47.32	100
2	1.38	1	0.28	8.1	27.73		9.02		5.36	47.14	100
2		1.01	0.27	8.66	30.17		9.74		3.89	46.26	100
3		1.16	0.21	8.66	30.81		10.11		2.56	46.5	100
3		0.88	0.44	8.37	28.94	0.18	9.22		6.35	45.62	100
3		0.86	0.27	8.4	30.08	0.19	10.52		3.71	45.97	100
4	1.6	0.98	0.21	8.53	28.85		9.32		2.38	48.13	100
4	1.85	1.03	0.23	8.23	27.67	0.16	9.04		3.96	47.83	100
4		0.91	0.42	8.66	28.66	0.18	9.29		6.31	45.57	100
5	1.88	1.02	0.32	8.27	28.25		9.38		2.7	48.19	100
5		0.97	0.37	8.73	29.79		10.05		4.01	46.07	100
5		1.07	8.88		30.59		10.36		2.7	46.4	100
6		1.04	0.3	9.13	30.78		9.84		2.19	46.71	100
6		1.19	0.26	8.98	29.72		9.54		4.16	46.16	100
6	2.15	0.88	0.23	7.91	28.04		9.94		2.55	48.3	100
7		0.98	0.66	8.75	28.74		9.38		5.78	45.7	100
7	2.33	0.92	0.39	7.44	24.83	0.15	8.25		8.62	47.08	100
7	1.97	1.18	0.25	8.31	27.97		9.21		2.9	48.21	100
8		1.07	0.35	8.98	30.47		10.21		2.47	46.45	100
8	1.87	0.76	0.31	8.1	27.48		9.03		4.65	47.8	100
8		0.65	0.87	8.09	27	0.24	8.89	0.21	9.38	44.67	100
9		0.99	0.51	8.33	28.23	0.2	8.8		7.6	45.33	100
9	1.62	0.94	0.48	8.19	27.62		8.6		4.94	47.6	100
9		1.05	0.33	8.64	29.33	0.22	9.83		4.83	45.77	100
10	3.27	0.8	0.34	7.67	26.34		9.18		3.12	49.27	100
10		0.79	0.46	8.48	29.85		10.65		3.83	45.95	100
10		0.84	0.46	8.57	30.04		10.35		3.63	46.11	100

Table 5. *Total organic carbon* (*%TOC*) *of the Dellen lithic impact breccia containing filaments* (*DL1*), *and of the crystalline target rock around Dellen* (*DG1*, *DG2*). *The annotations 'a' and 'b' after the sample name indicate duplicates of the same sample*

Sample	Description	TOC (%)
DL1 a	Lithic impact breccia containing filaments, Änga	0.42
DL1 b	Lithic impact breccia containing filaments, Änga	0.36
DG1 a	Crystalline target rock, Fredriksfors	0.18
DG1 b	Crystalline target rock, Fredriksfors	0.26
DG2 a	Crystalline target, Lenåsen	0.36
DG2 b	Crystalline target, Lenåsen	0.37

settings (e.g. Little *et al.* 1998; Thorseth *et al.* 2001; Emerson & Moyer 2002; Thorseth *et al.* 2003; Ivarsson *et al.* 2008). The semi-straight and coiled appearances (Figs 3(b) and (d)) (e.g. Little *et al.* 1998; Ivarsson *et al.* 2008), as well as the segmented (Figs 3(c), (d) and 5(b)) (e.g. Schumann *et al.* 2004; Ivarsson *et al.* 2008), branched (Figs 3(d) and 5(b)) (e.g. Little *et al.* 1998; Ivarsson *et al.* 2008), star-shaped (Fig. 3(c)) (e.g. Thorseth *et al.* 2001, 2003; Hofmann *et al.* 2008) and sheeted (Figs 4 and 5(a)) (e.g. Ivarsson *et al.* 2008) morphologies, correspond to morphologies of known filamentous microorganisms (e.g. Ehrlich 1996).

An alternative origin of the filaments is that they are formed abiogenically. The occurrence of the filaments in assemblages, or colonies, is consistent with a biologic origin, but assemblages could of course also be a result of abiologic mineral precipitation. However, abiologically formed filaments are more likely to be straight (Hofmann *et al.* 2008), i.e., not bended or twirled like the Dellen filaments. Branching is also a very typical feature of many simple filamentous microorganisms (i.e., Ehrlich 1996), although, during some circumstances, branching can also form abiogenically. Branching could, for example, be a result of inorganic self-organized mineral growth of ferric iron oxyhydroxide controlled by redox fronts in silica gel (Grenne & Slack 2003). Sheeted filaments, star-shaped filaments and segmented filaments are also very typical morphologies of simple microorganisms (Ehrlich 1996), and are widespread in microfossils of hydrothermal settings (e.g. Thorseth *et al.* 2001, 2003; Schumann *et al.* 2004; Hofmann *et al.* 2008; Ivarsson *et al.* 2008). However, similar morphologies have been created abiogenically in the laboratory (Kerr 2003; García-Ruiz *et al.* 2009). On the other hand, the abiogenic structures in these cases were grown from a medium at very different chemical

https://doi.org/10.1017/S147355041000011X Published online by Cambridge University Press

and physical conditions compared to the geological environment of a hydrothermal system.

The fibrous material on the filamentous structures could be interpreted as abiological mineral precipitates (Fig. 3(f)). Fungi, for example, are known to produce similar Ca-oxalates on their hyphae. Cross-sections examined in the ESEM show that these fibres originate almost in the centres of the filamentous structures and stretch out through both the inner and outer parts of the sheeted filaments (Fig. 4), and this rules out mineral precipitations on the surfaces as a possible explanation. The fibrous structures radiate 360° around the filaments. This is visible both in a petrographic microscope and the ESEM (Fig. 4). If the filaments have a biogenic origin, one explanation for these fibrous structures, other than being mineral precipitates, is that they are cilia. Cilia are used by various types of microorganisms, including bacteria, for movement in a fluid media. Beating of cilia creates currents in surrounding fluids that result in cell movement. Many fossilized microorganisms found in fractures and veins in hard rocks are usually attached to the vein walls (Ivarsson *et al*. 2008). The Dellen putative microfossils, on the other hand, are not attached to the vein walls or any mineral surface, but occur 'free' in the pore space while fluid circulation is active. Cilia are probably an advantage under such conditions by facilitating movement.

The setting of the filamentous structures, in a hydrothermal system, is compatible with a biologic origin of the filaments. Hydrothermal systems are known to harbour microorganisms and are considered as environments where microbial life thrives (Reysenbach & Cady 2001). The restriction of filaments to the fractured space indicates that the filaments only existed in the fractures and not in the surrounding rock. If the filaments were microorganisms, they probably lived in the system as long as hydrothermal fluids were circulating. As soon as the circulation ended and minerals formed, the putative microorganisms were trapped and preserved. However, the fracture and late mineral infilling of some of the putative microfossils show that the hydrothermal system was still active after the entrapment of the filaments.

Another possibility is that the filamentous structures in Dellen are a result of microorganisms that lived in the area before the formation of the impact structure, and were subsequently brought in by circulating fluids and preserved in the cracks of the impact breccia. Remnants of organisms could have subsequently been distributed through the cracks of the impact breccia by circulating hydrothermal groundwater.

The putative Dellen microfossils are indigenous with the rock, i.e., they are not a modern contaminant. The putative fossils are trapped and preserved in mineral phases that were formed by the hydrothermal activity. Further, the filaments are sometimes cut off by the fracture-filling hydrothermal alteration minerals (Fig. 5(b)). This shows that the filamentous structures were coexistent with the hydrothermal circulation fluids, and pre-dated the last hydrothermal fluid. Therefore, they are not a result of contamination by present-day microorganisms.

The irregular distribution of filamentous structures in relation to mineral surfaces is in favour of a biogenic origin, in contrast to an abiogenic origin (i.e., Peckmann *et al*. 2008). The filaments are independent of mineral surfaces, rims of early vein cementation or cleavage planes. Even if non-biogenic crystal growths may also occur independent of mineral surfaces rims of early vein cementation, or cleavage planes, mineral precipitates would generally be less randomly distributed than the biologically formed filaments.

Chemical composition

The chemical composition of the filamentous structures in Dellen, with a high Si and Fe content, is similar to the composition of microfossils in other hydrothermal settings (Al-Hanbali *et al*. 2001; Thorseth *et al*. 2001, 2003; Ivarsson *et al*. 2008; Peckmann *et al*. 2008). Silicification of microorganisms is a common and rapid fossilization process that favours preservation of the inner morphology, sometimes down to the cellular level (Toporski *et al*. 2002). The host rock of the Dellen filamentous structures is a granitic Si-rich rock, and the high Si content of the filamentous structures could reflect the silicification of microorganisms. Whether the filaments are biogenic or abiogenic, the high silica content could also simply be a result of a silicate-mineral precipitate. The high Fe content of the inner parts of the sheeted filamentous structures could reflect precipitation or deposition of iron in the microbial filaments. Hydrothermal fluids generally contain a high concentration of iron, which could have been dissolved from iron-bearing minerals in the target rock by the circulating fluids. This could have been the source of Fe^{2+} for possible Fe oxidation reactions. A high Fe content of microfossils has previously been explained by the involvement of microorganisms in Fe-oxidation reactions to gain energy for their metabolism (Ivarsson & Holm 2008). The filaments sometimes contain carbon and small amounts of chlorine, and so do other phases in the sample. The carbon content of the filaments cannot be used as an argument for biogenicity, since the glue of the polished sections contains carbon and chlorine, and when a block of the sample without glue was tested in the ESEM, only trace amounts of carbon were detected in the filaments. In addition, TOC analyses confirm that the sample as a whole contains only negligible amounts of carbon.

Colonization of the impact-generated hydrothermal system

If the putative microfossils are biogenic structures, the most likely scenario is that the microorganisms lived in the fractures while the hydrothermal system was active. The filaments are sometimes cut off by the hydrothermal alteration minerals, showing that they coexisted with the hydrothermal fluids. Once the fractures were sealed and filled with secondary minerals, the microorganisms were trapped and preserved. Since the Dellen structure is buried, and the samples of impact breccia are collected from loose blocks and boulders, it is not possible to say exactly where the sample containing putative microfossils is derived from within the crater. However, the occurrence of filaments in only one out of three

https://doi.org/10.1017/S147355041000011X Published online by Cambridge University Press

samples of impact breccia implies that the putative microfossils are restricted to a certain part of the crater. The habitable zones within an impact-generated hydrothermal system develop after cooling to suitable temperatures, which varies within different parts of the crater (Versh *et al*. 2006). The central uplift, for example, is the area that keeps the most favourable temperatures for microbial colonization for the longest period of time (Versh *et al*. 2006). Hydrothermal systems in impact craters are often suggested as settings that could harbour life. These systems are dynamic disequilibrium environments with a constant mixing of fluids and a flow of nutrients, which could be utilized by life as energy sources.

Conclusion

Based on similarities in morphology and composition to microfossils previously observed in hydrothermal deposits from other settings, we suggest that the most likely explanation for the filamentous structures in the Dellen lithic impact breccia is that they represent fossilized microorganisms. Our interpretation is that the microorganisms lived in the fractures while the hydrothermal system was active. Once the fractures were filled with secondary minerals the microorganisms were trapped and preserved.

This suggests that impact-generated hydrothermal systems are capable of supporting microbial life, and that evidence of this can be preserved in the geological record. Hence, impact-generated hydrothermal systems could be a potential target for the search for life on early Earth and Mars.

Acknowledgements

We are grateful to Marianne Ahlbom and Heike Siegmund for skilled technical support and to the Swedish National Space Board and the Knut and Alice Wallenberg Foundation for financial support. This manuscript benefited substantially by helpful criticism from the two reviewers.

References

Al-Hanbali, H., Sowerby, S.J. & Holm, N.G. (2001). *Earth Planet. Sci. Lett.* **191**, 213–218.

Ames, D.E., Watkinson, D.H. & Parrish, R.R. (1998). *Geology* **26**, 447–450.

Brock, T.D. (1978). *Thermophilic Organisms and Life at High Temperatures*. Springer, New York.

Corliss, J.B., Baross, J.A. & Hoffman, S.E. (1981). *Oceanol Acta* **Sp**, 59–69.

Corliss, J.B. *et al*. (1979). *Science* **203**, 1073–1083.

Dence, M.R., Grieve, R.A.F. & Robertson, P. (1977). Terrestrial impact structures: Principal characteristics and energy considerations. In *Impacts and Explosion Cratering*, ed. Roddy, D.J., Pepin, R.O. & Merill, R.B., pp. 247–276. Pergamon, New York.

Deutsch, A., Buhl, D. & Langenhorst, F. (1992). *Tectonophysics* **216**, 205–218.

Ehrlich, H.L. (1996). *Geomicrobiology*, 3rd edn, revised and expanded, p. 719. Marcel Dekker, New York.

Emerson, D. & Moyer, C.L. (2002). *Appl. Environ. Microbiol.* **68**, 3085–3093.

García-Ruiz, J.M., Melero-Garcia, E.M. & Hyde, S.T. (2009). *Science* **323**, 362–365.

Geptner, A.R., Ivanovskaya, T.A. & Pokrovskaya, E.V. (2005). *Lithol. Min. Resour.* **40**, 505–520.

Gibson, E.K., McKay, D.S., Thomas-Keptra, K.L., Wentworth, S.J., Westall, F., Steele, A., Romanek, C.S., Bell, M.S. & Toporski, J. (2001). *Precambrian Res.* **106**, 15–34.

Glamoclija, M., Schieber, J. & Reimold, W.U. (2007). Microbial signatures from impact-induced hydrothermal settings of the Ries crater, Germany; a preliminary SEM study. In *Proc. 38th Lunar and Planetary Science Conf*., Houston, Abstract 1989.

Grenne, T. & Slack, J.F. (2003). *Miner. Deposita* **38**, 625–639.

Henkel, H. (1992). *Tectonophysics* **216**, 63–89.

Hode, T., Cady, S.L., von Dalwigk, I. & Kristiansson, P. (2008). Evidence of ancient microbial life in an impact structure and its implications for astrobiology – a case study. In *From Fossils to Astrobiology*, ed. Sechbach, J. & Walsh, M., pp. 249–273. Springer, Netherlands.

Hofmann, B.A., Farmer, J.D., Von Blackenburg, F. & Fallick, A.E. (2008). *Astrobiology* **8**, 87–117.

Ivarsson, M. (2006). *Geochem. Trans.* **7**, 5.

Ivarsson, M. & Holm, N.G. (2008). Microbial colonization of various habitable niches during alteration of oceanic crust. In *Links between Geological Processes, Microbial Activities and Evolution of Life*, ed. Dilek, Y., Furnes, H. & Muehlenbachs, K., pp. 69–111. Springer Publications, Berlin.

Ivarsson, M., Lausmaa, J., Lindblom, S., Broman, C. & Holm, N.G. (2008). *Astrobiology* **6**, 1139–1157.

Jõeleht, A., Kirsimäe, K., Plado, J., Versh, E. & Ivanov, B. (2005). *Meteoritics Planet. Sci.* **40**, 21–33.

Kerr, R.A. (2003). *Science* **302**, 1134.

Lindström, M. & von Dalwigk, I. (2002). Part II: Dellen. In *Geological Guide to the Lockne and Dellen Impact Structures*, Stockholm contributions in geology, 47, pp. 33–45. Almquist & Wiksell International, Stockholm.

Little, C.T.S., Herrington, R.J., Maslennikov, V.V. & Zaykov, V.V. (1998). The fossil record of hydrothermal vent communities. In *Modern Ocean Floor Processes and the Geological Record*, Special Publications, 148, ed. Mills, R.A. & Harrison, K., pp. 258–270. Geological Society, London.

Naumov, M.V. (2002). Impact-generated hydrothermal systems: data from Popigai, Kara, and Puchezh-Katunki impact structures. In *Impacts in Precambrian Shields*, ed. Plado, J. & Peasonen, L.J., pp. 117–171. Springer, Berlin.

Newsom, H.E. (1980). *Icarus* **44**, 207–216.

Parnell, J., Bowden, S.A., Osinski, G.R., Lee, P., Green, P., Taylor, C. & Baron, M. (2007). *Geochim. Cosmochim. Acta* **71**, 1800–1819.

Parnell, J. *et al*. (2010). *Geology* **38**, 271–274.

Peckmann, J., Bach, W., Behrens, K. & Reitner, J. (2008). *Geobiology* **6**, 125–135.

Rathbun, J.A. & Squyres, S.W. (2002). *Icarus* **157**, 362–372.

Reysenbach, A-L. & Cady, S. (2001). *Trends Microbiol.* **9**, 79–86.

Schiffman, P. & Southard, R.J. (1996). *Clay. Clay Miner.* **44**, 624–634.

Schopf, J.W. (1999). *Fossils and pseudofossils: lessons from the hunt for early life on Earth*, pp. 88–93. Space Studies Board, National Research Council, Washington DC.

Schopf, J.W. & Walter, M.R. (1983). Archean microfossils: new evidence of ancient microbes. In *Earth's Earliest Biosphere, its Origin and Evolution*, ed. Scopf, J.W., pp. 214–239. Princeton University Press, Princeton, NJ.

Schumann, G., Manz, W., Reitner, J. & Lustrino, M. (2004). *Geomicrobiol. J.* **21**, 241–246.

Svensson, N.B. (1968). *Geologiska föreningens i Stockholm förhandlingar* (*GFF*) **90**, 314–316.

Thorseth, I.H., Pedersen, R.B. & Christie, D.M. (2003). *Earth Planet. Sci. Lett.* **215** 237–247.

Thorseth, I.H., Torsvik, T., Torsvik, V., Daae, F.L., Pedersen, R.B. & Keldysh-98 Scientific Party. (2001). *Earth Planet. Sci. Lett.* **194**, 31–37.

Toporski, J.K.W., Steele, A., Westall, F., Thomas-Keprta, K.L. & McKay, D.S. (2002). *Astrobiology* **2**, 1–26.

Utada, M. (2001). Zeolites in hydrothermally altered rocks. In *Natural Zeolites: Occurrence, Properties, Applications*, ed. Bish, D.L. & Ming, D.W., *Rev. Mineral. Geochem.* 45, 305–322.

Versh, E., Kirsimäe, K. & Joeleht, A. (2006). *Planet. Space Sci.* **54**, 1567–1574.